Displacement Evaluation on an Innovative Composite Reinforced Soil Structure

Vera Karla S. Caingles[1*], Maria Shahane L. Bual-Pono[2] and Cheryl F. Daleon[2]
[1]Department of Civil Engineering
University of Science and Technology of Southern Philippines – Cagayan de Oro
Cagayan de Oro City, 9000 Philippines
**vera.karla@ustp.edu.ph*

[2]Department of Civil Engineering
Central Mindanao University
Maramag Bukidnon, 8714 Philippines

Date received: March 25, 2024
Revision accepted: December 16, 2025

Abstract

Geosynthetic materials are widely used in civil engineering. Their application and evaluation are currently ongoing to better understand their behavior during design and construction. This study aims to assess the displacement behavior of a specially designed composite reinforced soil structure for innovative slope protection of riverbanks. Three prototypes were constructed for this study, each consisting of geogrid as the primary reinforcement and geotextile as the secondary reinforcement. The gravel drainage configurations included 0%, 50%, and 100%. The gravel used was 1-1/2"–2" sub-rounded gravel, and low plasticity silt (ML type) served as infill material. Horizontal displacement readings for each soil layer were recorded at the end of construction, when fully saturated, and after applying a 55 kPa surcharge load using horizontally installed rods and line gauges. The results indicated that all prototypes had horizontal displacements below the recommended threshold of 4%, consistent with Federal Highway Administration (FHWA) performance criteria and AASHTO design principles. The prototype without gravel drainage showed the lowest average displacement percentage among all. Therefore, the innovative composite-reinforced soil structure can serve as an alternative slope-protection method for riverbanks. It is advisable to design a conservative anchorage system to prevent deviations between initial and final positions, and to explore additional design variables to enhance the performance of this innovative structure.

***Keywords**:* displacement analysis, geotechnical engineering, laboratory testing quantitative approach, Philippines

1. Introduction

The application and construction of geotechnical structures such as retaining walls, piled embankments, and others are increasing significantly worldwide. This growth is driven by the booming economies of countries where infrastructure is developed to support regional development and societal needs. Additionally, some structures are designed to protect the environment and communities from damage caused by natural geological hazards, such as landslides and erosion. Soil plays a central role in landslides and erosion, making it a challenge for geotechnical and civil engineers to obtain precise data on soil properties. This information is essential for designing structures that can resist damage from natural hazards and ensuring that they are built on safe, stable soil. Moreover, many geotechnical researchers have investigated various soil properties and identified factors that influence changes in soil behavior.

Meanwhile, different techniques and methods for ground improvement have been tested to increase soil performance in terms of soil bearing capacity, stability, settlement, sliding, shear resistance, suppress lateral deformations, improve stiffness, and increase elastic modulus (Bergado *et al*., 1996; Pokharel *et al*., 2009; Hejazi *et al*., 2012; Morsy *et al*., 2020; Szymanski *et al*., 2021; Khan *et al*., 2024; Sharma *et al*., 2024). These techniques include removal and replacement, vertical drains, pre-compression, grouting, in-situ densification, stabilization using admixture and reinforcement, compaction piles, the lime or cement deep-mixing method, and mechanically stabilized earth embankments (Bergado *et al*., 1996). Among all the techniques, soil reinforcement is the most common technique for ground improvement. Its advantages include ease of construction, low construction costs, and time savings. It is a ground improvement technique that uses natural and synthetic materials to advance the engineering properties and performance of soil. In recent decades, the use of geosynthetics to reinforce and stabilize soil and other earthen structures, such as landfills, embankments, slopes, and retaining walls, has been widely practiced in engineering. Generally, geosynthetics comprise synthetic polymers such as polyamide, polyvinyl chloride, and polypropylene. Hence, due to its composition, it has high resistance to biological and chemical degradation. Geosynthetics also have a wide range of applications in almost all civil engineering fields, such as geotechnical, environmental, coastal, and hydraulic engineering (Shirsath and Choudhari, 2018). Furthermore, the application of this material has resulted in a significant increase in the safety factor, improved construction material

performance, and reduced construction costs compared with conventional design (Koerner, 1998; Holtz *et al*., 1997).

The Philippines is on the path of tropical cyclones. Thus, the country incurs substantial damage from flooding following heavy rainfall. News bulletins showed damaged houses along the Marikina Riverbank in 2016 (GMA News, 2016); collapsed houses along the creek in Caloocan City in 2015 (GMA News, 2015); failed portion of flood control protection at Barangay Barra, Opol, Misamis Oriental in 2016; and the failed riprap as riverbank protection in Zamboanga City in 2019 (Climaco, 2019). Local officials reported that the riverbank protection failed during or after prolonged rainfall. Hence, it is important to have mitigating measures to prevent such occurrences.

The emergence of geosynthetics technology, which includes geotextiles, geonets, geomembranes, geogrid, and geocell, offers and provides more manageable, flexible, cost-efficient, and environmentally acceptable methodology to address the ongoing challenges in construction and on the environment (Reddy *et al*., 2018; Rawi and Abade, 2017); Sharma and Goliya, 2014; Khan and Saran, 2006; Guler and Ocbe, 2003). Today, geosynthetics-reinforced earth structures are widely recognized for their cost-effectiveness and environmental sustainability. The mechanically stabilized earth (MSE) or reinforced earth (RE) technique is the most commonly used and constructed soil retaining system (Reddy *et al*., 2018). This is due to its flexible features, which include enclosed reinforcements and aesthetically finished block walls. Another advantage of MSE is its economic benefits, as it requires less site preparation, requires less space, and can stabilize heights of more than 30m (Soleimanbeigi, 2016). It can lead to up to 50% savings in construction costs (Bergado *et al*., 1996; Circulado and Lorenzo, 2020), as well as in the wall heights (Koerner and Koerner, 2011). Anchored in this concept, the researchers evaluated the displacement behavior of the designed composite-reinforced soil structure as an innovative slope-protection structure for the riverbank, considering the reinforcing-confining-drainage mechanism.

1.1 Research Objectives

This research aims to address a gap in the existing literature by providing a more comprehensive evaluation of the displacement behavior of composite-reinforced soil structures as an innovative slope-protection structure for riverbanks, considering the reinforcing-confining-drainage mechanism. Specifically, it aims to: determine the physical properties of the soil and coarse

aggregates as the filling and gravel drainage materials, respectively (a); determine and evaluate the displacement behavior of the prototypes with drainage path and varying intermediate gravel drainage of 0%, 50%, and 100% at the end of construction (EOC), under fully saturated condition (FSC), and total surcharge loading (TSL) of 55 kPa (b); and determine the maximum capacity of the 100% gravel drainage prototype following the 4% performance-based criteria outlined by the Federal Highway Administration (FHWA) and in alignment with AASHTO design principles (c).

2. Methodology

This research employed a uniaxial geogrid and a continuous, needle-punched nonwoven geotextile. The geogrid is the primary reinforcement, while the geotextile serves as the secondary reinforcement as a separator medium between the infill soil interface and aggregate drainage. The infill and backfill soils were delivered to AC Joyo Design & Technical Services Inc. in Davao City to undergo laboratory tests which adheres to the American Society for Testing and Materials (ASTM) standard including grain size analysis (ASTM D6913/D6913M), Atterberg limit (ASTM D4318), specific gravity (ASTM D854), compaction (ASTM D1557), and direct shear (ASTM D3080/D3080M). Sub-angular gravel was used as the intermediate horizontal drainage and back drainage, and as the facing of the prototypes. The gravel size ranges from 1-1/2" to 2". The gravel properties, including bulk density and specific gravity, were determined using Standard Test Method for Bulk Density and Voids in Aggregate (ASTM C29) and Standard Test Method for Relative Density and Absorption of Coarse Aggregate (ASTM C127). These tests were conducted at the Quality and Assurance Section Laboratory of the Department of Public Works and Highways- Misamis Oriental in El Salvador City, Misamis Oriental.

The design concept for the prototypes was based on studies by Elias *et al*. (2001) and Koerner (1998). The geogrid shear stress interaction coefficient ranged from 0.7 to 0.8. The prototypes' dimensions were 1.8 m × 1.2 m × 2.4 m (L × W × H), with a geogrid reinforcement length of 1.30 m and a uniform spacing of 0.40 m. The design criteria required for the prototype are shown in Table 1.

Table 1. Design criteria (FHWA NHI-00-043 (Elias *et al*., 2001)

Factor of Safety	External Stability Equations	
Sliding	$FS_{sliding}$	$= \frac{\Sigma\ Horizontal\ Resistance\ Forces}{\Sigma\ Horizontal\ Sliding\ Forces} \geq 2.0$
Overturning	$FS_{overturning}$	$= \frac{\Sigma\ Resisting\ Moment}{\Sigma\ Driving\ Moment} \geq 1.0$
Bearing Capacity	$FS_{bearing}$	$= \frac{q_{ult}}{q_{actual}} \geq 1.0$
	Internal Stability Equations	
Tensile Failure	$FS_{rupture}$	$= \frac{T_{allow}}{T_{max}}$
Pullout Failure	$FS_{pullout}$	$= \frac{T_{pullout}}{T_{max}}$

where:

$T_{allow} = \frac{T_{ult}}{CRF} = \frac{T_{ult}}{RF_{CR}\ x\ RF_{ID}\ x\ RF_{CD}\ x\ RF_{BD}}$ $T_{max} = K\sigma_v S_v(FS_{eq})$

$T_{pullout} = 2C_i C_r L_e \sigma_v tan\ \phi'_{fill}$ K = *earth pressure coefficient*

RF = *reduction factor* σ_v = *vertical earth pressure*

C_i = *pullout interaction coefficient* L_e=*effective length of embedment*

C_r = *coverage ratio* ϕ'_{fill} = *friction angle of filling*

Moreover, the designed prototypes incorporated an integrated facing-wall barrier, embedded reinforcements, intermediate gravel drainage layers, and a back drain. The primary reinforcement of the prototype was the geogrid, while the secondary reinforcement and separating medium between the infill soil and gravel drainage was the geotextile. It had three intermediate gravel drainage configurations: no gravel drainage, half gravel drainage at 0.65 m, and complete gravel drainage at 1.3 m. The intermediate gravel drainage and the facing and back drains had thicknesses of 75 mm and 100 mm, respectively. Figure 1 presents the elevation view of the three prototypes. A reinforced rectangular tank with the following measurements, 2.7 m height, 3.0 m length, and 1.5 m width, was used to encase the field prototypes. Figure 2 shows the actual photo with dimensions of the test tank and the prototype.

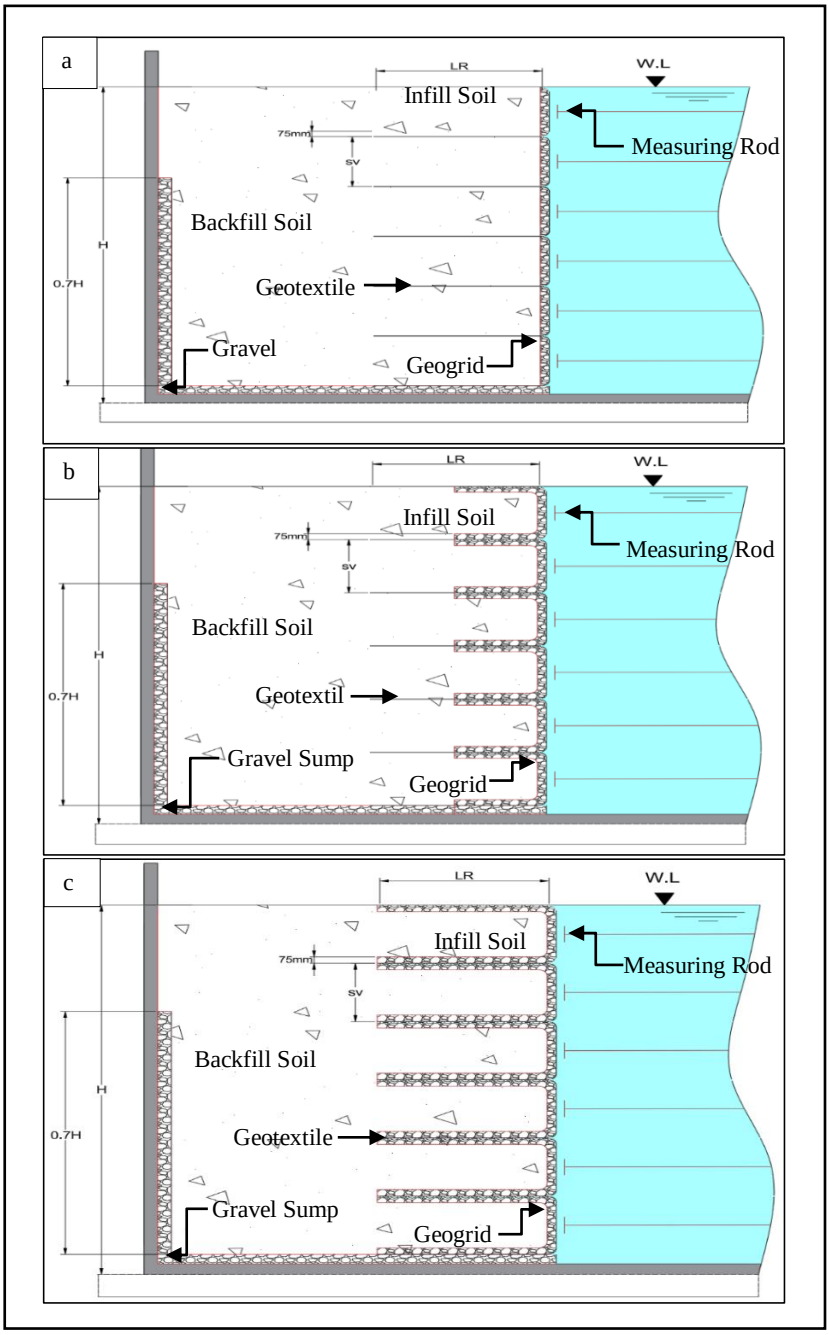

Figure 1. Prototypes with varying intermediate at 0% drainage at 0% (a), 50% drainage (b), and 100% drainage (c)

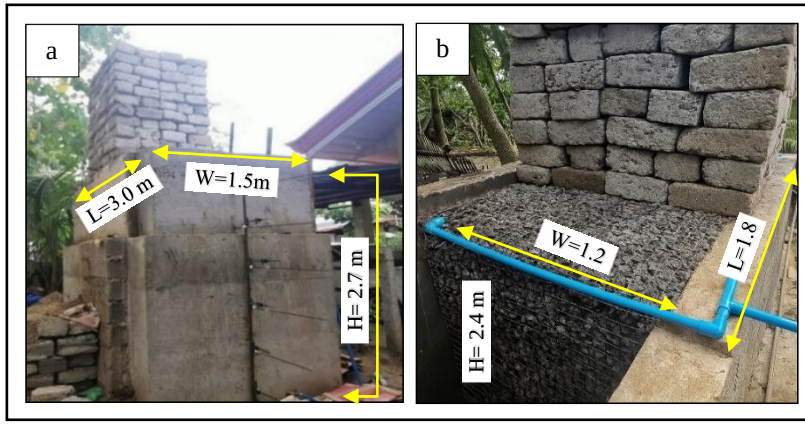

Figure 2. Dimensions of the Test tank: outer (a) and inner (b)

2.1 Instrumentation

The evaluation of the displacement of the prototypes was taken from the installed horizontal rods inside the tank, placed at the center of every layer, extending to the exterior walls, where line gauges from a digital caliper were installed.

2.2 Construction of Prototype

The soil materials, such as backfill and infill, were prepared at their optimum moisture content. The soil was compacted in accordance with ASTM D698, using a 20 kg steel tamper and maintaining a constant drop height of 400 mm. The calculated compaction effort for the study was 600 kN · m/m^3. The construction of the prototypes followed a systematic procedure. First, a thin layer of soil was placed at the bottom part of the prototype to increase friction between the prototype and the tank. Second, a geogrid sheet was placed on the top of the soil. Third, the intermediate and back gravel drainage were constructed with a thickness of 75 mm and 100 mm, respectively. Fifth, the geotextile was placed on the top of the gravel, followed by the uniformly compacted infill soils. Six, the placement of the geotextile on top of the infill soils to separate the next layers of aggregates and the infill soil. The facing section was then filled with coarse gravel. It was covered by the geogrid as its protective layer and served as the primary reinforcement. This process was repeated up to a height of 2.4 m of the prototype. The process was then repeated until the prototype reached a height of 2.4 m. To avoid any movement of materials inside the prototype, a temporary facing board was placed

however, it was then removed after the installation of the last layer. Figure 3 displays the components of the prototype.

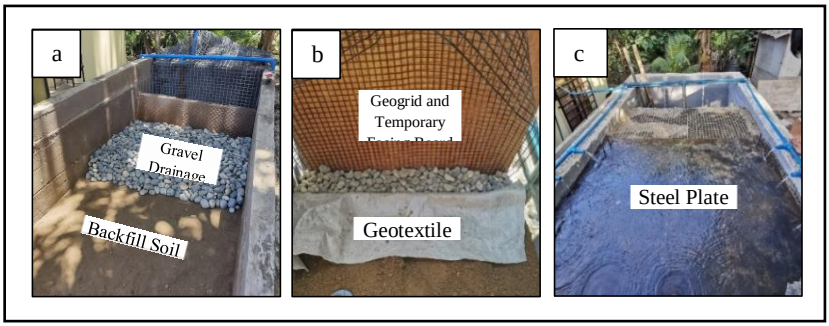

Figure 3. Main components of the prototype: compacted backfill soil and laying of gravel for drainage (a); placement of the temporary facing board and geotextile (b); and submerged prototype with steel plate for even distribution of vertical loading (c)

2.3 Prototype Testing

After removal of the temporary facing board, the end-of-construction (EOC) initial lateral displacement readings were recorded. Figure 4 shows a prototype filled with water, used to immerse materials for 48 hours to achieve full saturation. Then, the water was drained, and the second lateral displacement readings for the fully saturated condition (FSC) were documented. Moreover, the following procedure was the application of incremental surcharge loading. Two (2) layers of concrete blocks were placed on top of the prototype, and the prototype was then filled with water for three (3) hours. After the water was drained, the lateral displacement was recorded. These steps were done until the 11 layers were loaded. The equivalent load of these blocks was 55 kPa. Figure 5 shows the actual loading of the concrete blocks.

Figure 4. The prototype was immersed in water inside the test tank to achieve full soil saturation

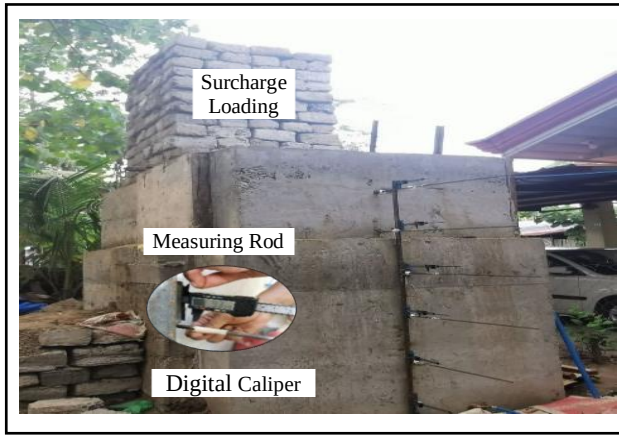

Figure 5. Full surcharge loading of 55 kPa was applied in the prototype

3. Results and Discussion

The percentages of particle sizes of the infill and backfill materials used in this study as shown in Table 2. The materials consist mainly of fine-grained soil (approximately 88%) and a smaller amount of coarse-grained soil. Moreover, the results of the physical property tests show that the soil had a specific gravity of 2.5, a liquid limit of 34.93%, a plastic limit of 31.49%, and a plasticity index of 3.44%. The coefficient of uniformity was recorded to be

11.62, while the coefficient of concavity was 0.61. The maximum dry density (MDD) and optimum moisture content (OMC) were 1597.5 kg/m^3 and 21.40%, respectively. The values of cohesion and friction angles were 6.453° and 71.5 kPa, respectively. A summary of the properties of the infill and backfill soil material is shown in Table 3. The properties of the coarse aggregates are shown in Table 4. The specific gravity recorded was 2.65, while the loose and compacted densities of the gravel material were 1535.34 kg/m^3 and 1663.51 kg/m^3, respectively.

Table 2. Percent by mass of soil samples

Type	Size	Percent
Gravel	> 4.75 mm	0%
Sand	4.75 mm to 0.075 mm	12%
Clay and Silt	0.075 mm to < 0.005 mm	88%

Table 3. Summary of infill and backfill soil properties

Property	Value	Property	Value
Soil Classification	Silt (ML)	Specific Gravity (S.G)	2.50
Liquid Limit (L.L)	34.93	Optimum Moisture Content	21.40 %
Plastic Limit (P.L)	31.49	Maximum Dry Density	1597.5 kg/m^3
Plasticity Index (P.I)	3.44	Friction angle	6.453°
		Cohesion	71.5 kPa

Table 4. Coarse Aggregate Properties

Property	Value	Property	Value
Particle Size	1-1/2”-2”	Loose Density	1535.34 kg/m^3
Specific Gravity	2.65	Compacted Density	1663.51 kg/m^3

3.1 Displacement of Prototypes at the End of Construction (EOC)

After the EOC, the bottom layer of all the prototypes exhibited the highest displacement: 0.61% for prototype 1 (no-gravel drainage prototype), 1.08% for prototype 2 (half-gravel drainage prototype), and 1.38% for prototype 3 (full-gravel drainage prototype). The lowest displacement occurred at 0.42H for prototypes 1, 2, and 3, which were 0.17%, 0.37%, and 0.72%, respectively. A considerable displacement was also recorded at the top of each prototype: 0.45% for prototype 1, 0.81% for prototype 2, and 1.37% for prototype 3. The maximum displacement documented for the intermediate layers of each

prototype occurred at 0.25H, which was 0.51% for prototype 1, 1.05% for prototype 2, and 1.32% for prototype 3. Moreover, the average lateral displacement of the three prototypes at the EOC was 0.39% for prototype 1, 0.75% for prototype 2, and 1.08% for prototype 3. The trend clearly shows that greater drainage content led to increased lateral displacement, likely due to reduced soil confinement and internal settlement within the gravel layers. In the full-drainage configuration (Prototype 3), the loose interface between soil and drainage media may have allowed for more deformation under minimal surcharge conditions. Figure 6 shows graph of the relationship between normalized lateral displacement and height of the prototype at the EOC.

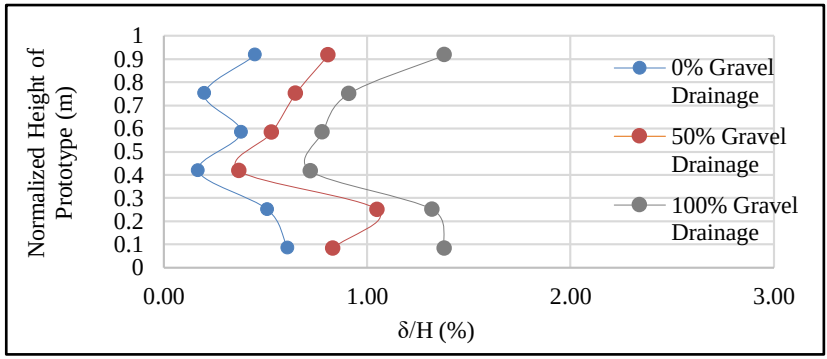

Figure 6. Normalized lateral displacement vs prototype height at the EOC

3.2 Fully Saturated Condition Displacement of the Prototypes

The prototypes were fully immersed in water for 48 hours. Moisture content was determined after the water was drained. The results showed that all prototypes achieved full saturation. Figure 7 demonstrates the relationship between the normalized lateral displacement and prototype height after 48 hours of water immersion. The highest lateral displacements were 1.48% for prototype 1, 1.58% for prototype 2, and 2.07% for prototype 3. These were observed at the bottom layer of the prototypes. The lowest displacements for prototypes 1 and 2 were 0.42H (0.39%) and 0.40H (0.40%), respectively, whereas the lowest displacement for prototype 3 was 0.58H (1.20%). It was observed that the top layer of prototype 1 had a relatively small increase in displacement compared to the other prototypes. The recorded top-layer displacement for prototype 1 was 0.47%, for prototype 2 0.98%, and for prototype 3 1.45%. The location of the highest displacement among the intermediate layers of the prototypes remained consistent with the EOC

observations at 0.25H. The displacements at 0.25H were 1%, 1.23%, and 1.57% for prototypes 1, 2, and 3, respectively.

This reaffirms the tendency of partially confined areas to act as stress transition zones, where material interface behavior, particularly between soil and gravel, influences structural movement under moisture-induced weakening.

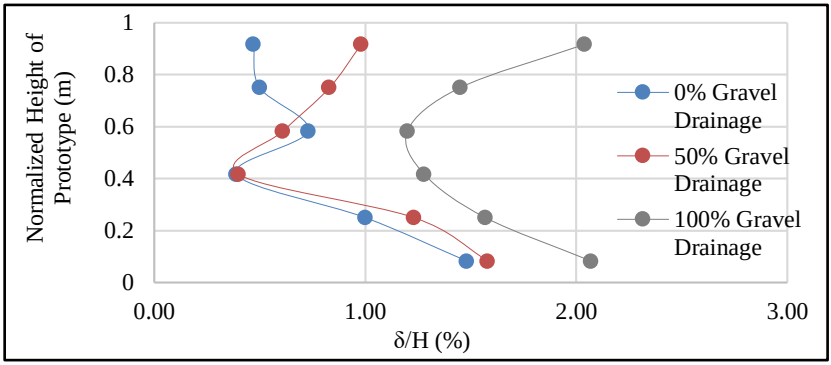

Figure 7. Normalized lateral displacement vs prototype height at the FSC

3.3 Displacement of Prototypes at Total Surcharge Loading of 55 kPa

To determine the lateral displacement under total surcharge loading, concrete blocks were loaded on the topmost layer of each prototype until a total applied stress of 55 kpa was reached. The applied stress was twice the prototype's designed capacity. The maximum lateral displacement remained consistent with that of FSC, which was located in the bottom layer of the three prototypes. The recorded displacements at the bottom layer were 1.90%, 2.13%, and 3.99% for prototypes 1, 2, and 3, respectively. This trend reinforces the effect of gravel drainage on confinement loss: more gravel results in looser soil structure and greater deformation under vertical loading. The results showed that the intermediate layers consistently moved from FSC to TSL. The lowest displacement occurred at 0.42 H for prototypes 1 and 2, which were 1.12% and 1.15%, respectively. The lowest displacement for prototype 3 occurred at 0.75 H, which was 3.41%. The shift in minimum displacement location for Prototype 3 may indicate a more uniform loss of stiffness throughout the height due to excessive drainage and insufficient confinement. The recorded top layer displacement was 1.39% for prototype 1, 2.08% for prototype 2, and 3.98% for prototype 3. This pattern indicates that

as drainage volume increased, structural flexibility and susceptibility to outward deformation at the least-confined sections also increased. Figure 8 displays the normalized lateral displacement vs. prototype height at TSL. In evaluating the average horizontal displacement after TSL, prototype 1 had the lowest value at 1.38%. Meanwhile, prototype 2 had an average displacement of 1.77%, and prototype 3 had 3.86%, twice that of prototype 2.

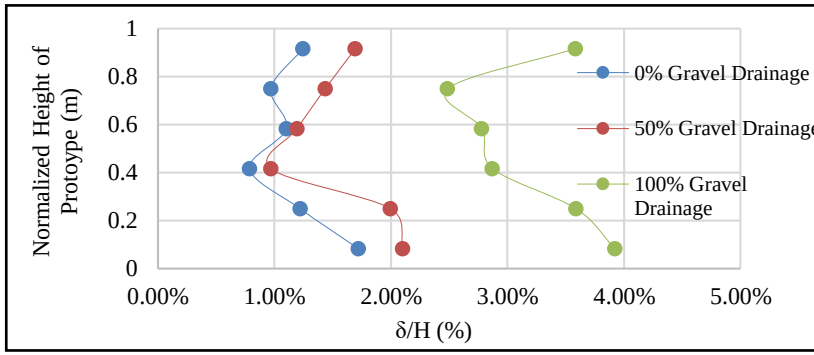

Figure 8. Normalized lateral displacement vs prototype height at TSL

3.4 Maximum Surcharge Loading of 100% Gravel Drainage Prototype, Considering 4% Maximum Displacement

The prototype was subjected to a total of 13 layers of concrete blocks, resulting in 60.83 kPa applied pressure to ascertain the maximum surcharge loading that the 100% gravel drainage prototype can accommodate before reaching the 4% permissible displacement limit recommended by the performance-based criteria outlined by the Federal Highway Administration (FHWA) and in alignment with AASHTO design principles under LRFD Bridge Design Specifications by AASHTO (2020). Figure 9 shows the normalized lateral displacement versus prototype height for the 100% gravel drainage prototype up to 4% displacement. The maximum displacement occurred at the top layer and at 0.25 H of the prototype (4.13%), whereas the lowest displacement occurred at 0.75 H (3.55%). The average lateral displacement of the prototype is computed as 4.00%; thus, an applied stress of 60.83 kPa, which is equivalent to 13 layers of blocks (12 layers and 6 blocks) weighing a total of 5886 kg, is the maximum applied surcharge loading that the prototype can withstand considering the 4% displacement limit.

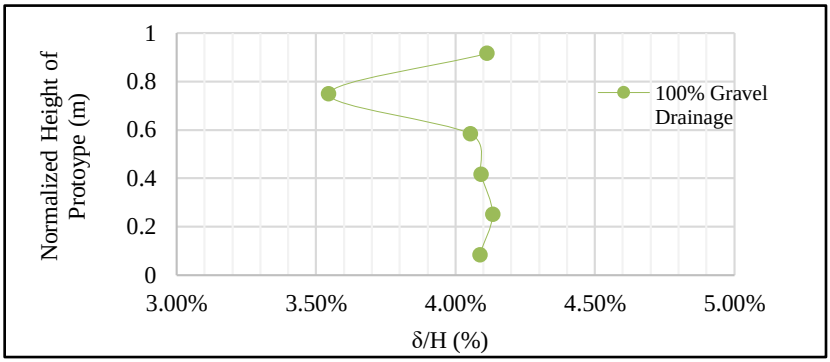

Figure 9. Normalized Lateral Displacement vs. Prototype Height of 100% Gravel

3.5 Average Lateral Displacements

To further assess and compare the overall behavior and performance of the prototypes under various conditions, the average lateral displacements were computed, and significant differences were assessed. The average lateral displacement of the three (3) prototypes is shown in Table 5.

Table 5. Average Lateral Displacement of the Prototypes

Prototype (% Gravel Drainage)	EOC	Rank	FSC	Rank	TSL	Rank
0% (Prototype 1)	0.39%	3	0.76%	3	1.38%	3
50% (Prototype 2)	0.71%	2	0.94%	2	1.77%	2
100% (Prototype 3)	1.08%	1	1.70%	1	3.86%	1

Analysis of variance (ANOVA) in SPSS was used to evaluate significant differences in the displacements of composite-reinforced soil-structure prototypes at the end of construction (EOC), in the fully saturated condition (FSC), and under total surcharge loading (TSL). The significant differences for all three conditions (EOC, FSC, TSL) are shown in Table 6.

Table 6. ANOVA for Composite Reinforced Soil Structure Lateral Displacement

SINGLE FACTOR ANOVA					
Displacement at EOC					
	Sum of Squares	df	Mean Square	F	Sig.
Between Groups	1.445	2	0.722	11.754	< 0.001
Within Groups	0.922	15	0.061		
Total	2.366	17			
Displacement at FSC					
	Sum of Squares	df	Mean Square	F	Sig.
Between Groups	2.337	2	1.169	7.103	0.007
Within Groups	2.468	15	0.165		
Total	4.805	17			
Displacement at TSL					
	Sum of Squares	df	Mean Square	F	Sig.
Between Groups	21.299	2	10.650	95.796	< 0.001
Within Groups	1.668	15	0.111		
Total	22.967	17			

The results in Table 7 revealed no significant differences between prototype 1 and prototype 2, or between prototype 2 and prototype 3. However, it showed a significant difference between prototype 1 and prototype 3. The mean difference in average lateral displacement was 0.693%, and the p-value for the difference between prototypes 1 and 3 was 0.001, significant at the 0.05 alpha level. It can be inferred that prototype 1 yielded the lowest displacement before saturation, whereas prototype 3 yielded the highest displacement. Therefore, the effect of the horizontal gravel drainage on the reinforced earth system was similar to all prototypes at EOC.

Table 7. Multiple Comparisons of Composite Reinforced Soil Structure at EOC

Multiple Comparisons						
(I) Prototype	(J) Prototype	Mean Difference (I-J)	Std. Error	Sig.	95% Confidence Interval Lower Bound	95% Confidence Interval Upper Bound
1.00	2.00	-.32167	.14313	.095	-.6934	.0501
	3.00	-.69333*	.14313	.001	-1.0651	-.3216
2.00	1.00	.32167	.14313	.095	-.0501	.6934
	3.00	-.37167	.14313	.050	-.7434	.0001
3.00	1.00	.69333*	.14313	.001	.3216	1.0651
	2.00	.37167	.14313	.050	-.0001	.7434

**The mean difference is significant at the 0.05 level*

Subsequently, the average lateral displacement of the prototype at fully saturated conditions (FSC) is shown in Table 8. The findings revealed a

significant difference between prototypes 2 and 3, with a mean difference of -0.658% (p = 0.033), which was significant at the 0.05 alpha level. Also, prototypes 1 and 3 showed a significant difference, similar to the EOC condition, with a mean difference of 0.838% and a p-value of 0.007, which was significant at the 0.05 alpha level. Prototypes 1 and 2 exhibited no substantial changes. It can be inferred that prototype 1 yielded the lowest value, while prototype 3 yielded the highest displacement value.

Table 8. Multiple Comparisons of Composite Reinforced Soil Structure at FSC

Multiple Comparisons						
(I) Prototype	(J) Prototype	Mean Difference (I-J)	Std. Error	Sig.	95% Confidence Interval Lower Bound	95% Confidence Interval Upper Bound
1.00	2.00	-.18000	.23418	.727	-.7883	.4283
	3.00	-.83833*	.23418	.007	-1.4466	-.2301
2.00	1.00	.18000	.23418	.727	-.4283	.7883
	3.00	-.65833*	.23418	.033	-1.2666	-.0501
3.00	1.00	.83833*	.23418	.007	.2301	1.4466
	2.00	.65833*	.23418	.033	.0501	1.2666

**The mean difference is significant at the 0.05 level*

The data in Table 9 disclosed a significant difference between prototypes 1 and 3 and prototypes 2 and 3 at total surcharge loading. The mean difference between prototypes 1 and 3 is 2.478% with a p-value of less than 0, which was significant at 0.05 alpha, while the mean difference between prototypes 2 and 3 was -2.087% with a p-value of less than 0, which was significant at 0.05 alpha. It can be inferred that the prototype without gravel drainage had lower displacement than the prototypes with gravel drainage.

Table 9. Multiple Comparisons of Composite Reinforced Soil Structure at TSL

Multiple Comparisons						
(I) Prototype	(J) Prototype	Mean Difference (I-J)	Std. Error	Sig.	95% Confidence Interval Lower Bound	95% Confidence Interval Upper Bound
1.00	2.00	-.39167	.19250	.138	-.8917	.1084
	3.00	-2.47833*	.19250	.000	-2.9784	-1.9783
2.00	1.00	.39167	.19250	.138	-.1084	.8917
	3.00	-2.08667*	.19250	.000	-2.5867	-1.5866
3.00	1.00	2.47833*	.19250	.000	1.9783	2.9784
	2.00	2.08667*	.19250	.000	1.5866	2.5867

**The mean difference is significant at the 0.05 level*

3.7 Prototype 1 (0% Gravel Drainage) Displacement Behavior

Figure 10 shows the graph of the displacement behavior of prototype 1 (0% Gravel Drainage). It demonstrated consistently stable performance throughout the three test phases. Between the End of Construction (EOC) and the Fully Saturated Condition (FSC), the topmost layer had a significant movement, while the bottom layer had a slight movement. This indicates that the soil layers near the surface were initially well confined. In contrast, the bottom layer exhibited greater movement due to water infiltration and softening of the underlying soil strata. In contrast, from the FSC to the Total Surcharge Loading (TSL) phase, the bottom layer exhibited minimal additional displacement, whereas the topmost layer showed greater displacement. This reversal in displacement behavior implies that the surcharge load had a greater impact on the upper layers once the system was fully saturated and the pore water pressure had dissipated. The maximum displacement under TSL was 1.90%, occurring at the bottom layer. Average displacement deviations across the three conditions were 0.37% from EOC to FSC and 0.62% from FSC to TSL, indicating a progressive but controlled increase in lateral movement. The total displacement from EOC to TSL was highest at 0.08H (1.29%) and lowest at 0.25H (0.88%), resulting in an average displacement deviation of 0.99%. These results demonstrate the beneficial effect of confinement without drainage, which reduces internal deformation. Compared with Prototypes 2 and 3, Prototype 1 demonstrated greater structural stability, indicating that reduced drainage may enhance confinement and mitigate excessive lateral displacement.

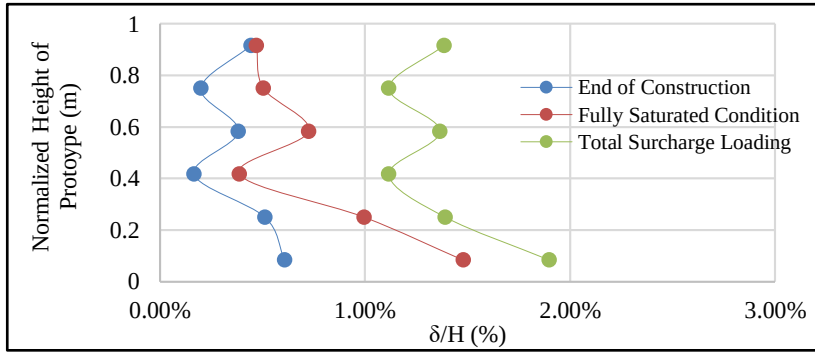

Figure 10. Prototype 1 displacement behavior graph

3.8 Prototypes 2 and 3 Displacement Behavior

Figure 11 shows the graph of the displacement behavior of prototype 2, which has a 50% intermediate gravel drainage configuration. From the End of Construction (EOC) to Fully Saturated Condition (FSC), the topmost layer showed a consistent slight movement in position, suggesting that there is a sufficient initial confinement, while the bottom layer showed a considerable change in position, possibly due to localized softening resulting from partial water accumulation within the drainage zone. As the system transitioned from FSC to Total Surcharge Loading (TSL), both the top and bottom layers showed further increase in displacement. This suggests that the partial drainage configuration may have introduced heterogeneity in the structure's stiffness profile, resulting in strain concentration zones under increased loading. The average total movement of prototype 2 from EOC to TSL was 1.06%. The maximum displacement of prototype 2 was recorded at 0.25H under TSL, which was 2.20%. Compared with prototype 1, prototype 2 exhibited smaller deviations from EOC to FSC in most layers, except in the top layer. These results indicate that although 50% gravel drainage configuration offered some drainage benefits, it did not sufficiently counteract the destabilizing effects of water ingress and surcharge.

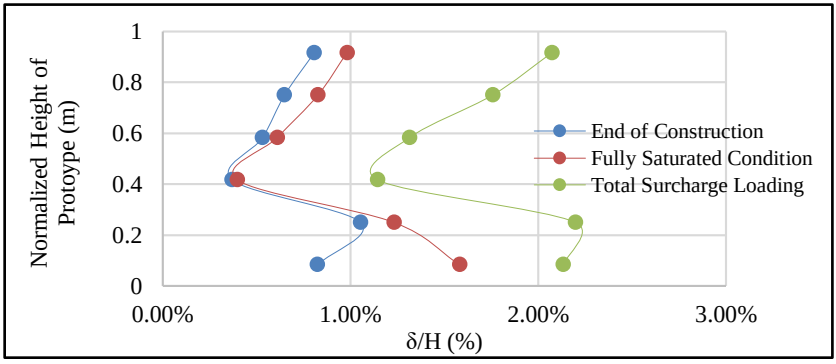

Figure 11. Prototype 2 Displacement behavior graph

Figure 12 shows the graph of the displacement behavior of prototype 3 with 100% gravel drainage configuration. From the End of Construction (EOC) to the Fully Saturated Condition (FSC), the average displacement was 0.52%. However, displacement has increased notably from FSC to Total Surcharge Loading (TSL), with an average displacement of 2.26%. This substantial increase of displacement indicates that the full gravel drainage configuration, while beneficial for water flow, may have reduced overall soil confinement,

creating instability during the application of loading. The maximum deviation occurred at the bottom of the prototype at 1.38% for EOC, 2.07% for FSC, and 3.99% for TSL. Moreover, the minimum deviation occurred at 0.42H for EOC (0.72%), whereas for the FSC and TSL, the locations were 0.58H (1.20%) and 0.75H (3.81%), respectively. From EOC to TSL, the average total displacement was 2.78%. These results suggest that the full gravel drainage configuration may have introduced excessive internal voids, thereby facilitating lateral soil movement. Additionally, water saturation likely caused fine soil particles to migrate through the geotextile into the drainage zone, reducing the overall fill mass and structural integrity of the structure. This mechanism is consistent with findings by Koerner and Koerner (2011), who noted that insufficient filtration and overdesigned drainage can act as failure planes rather than reinforcement zones.

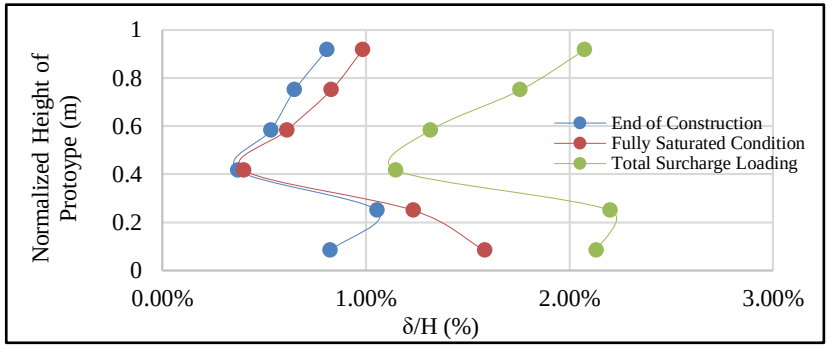

Figure 12. Prototype 3 displacement behavior graph

4. Conclusion and Recommendation

This study demonstrated that displacement behavior in composite geosynthetic-reinforced soil structures is significantly affected by the configuration of gravel drainage layers. The maximum displacement was noticed at the bottom layer of the three prototypes after the total surcharge loading. The highest lateral movement was observed at prototypes 1, 2, and 3 were 1.72%, 2.10%, and 3.99%, respectively. These data indicated that the bottom layer of the prototypes had experienced sliding, and the highest lateral movement was observed at prototype 3 with full-gravel drainage. Moreover, there was a noticeable deviation at the topmost layer among the prototypes from the initial to final position. For the intermediate layers, the maximum

displacement of the prototypes occurred at 0.2H. In addition, a structural bulge was observed, particularly in the prototypes with gravel drainage, which showed significant positional change from EOC to FSC. It implied that the presence of water significantly influences the displacement behavior of each layer of the prototype. Based on the displacement results, prototype 3 with full-gravel drainage had the highest average total displacement, followed by prototype 2 and then prototype 1. The movement of the gravel drainage prototypes indicated that water infiltration through the soil mass would pass the very fine soil particles through the geotextile material. In effect, the quantity of the infill soil was reduced, resulting in structural movement. These findings suggest that optimal design must balance drainage effectiveness with soil retention and mechanical confinement. Finally, the average and individual displacements of all prototypes were below the 4% permissible limit as outlined by the Federal Highway Administration (FHWA) and consistent with AASHTO design principles. Hence, the designed innovative composite reinforced soil structure could be an alternative slope protection for the riverbank. This research contributes valuable insights for the practical design of reinforced earth systems in real-world settings, such as flood-prone riverbanks, highways, and embankment slopes, especially in tropical regions like the Philippines.

5. Acknowledgement

Special thanks to the people for their support in completing this study: Engr. Jerald Kier S. Pono, Sgt. Glenn L. Bual, Mrs. Aida L. Mapa, Mr. and Mrs. Bual, Mr. Herberto C. Sencio, Mr. Teody Patac, AC Joyo Design & Technical Services Inc., all skilled laborers, and to our Almighty God for the strength and wisdom given to complete this research study.

6. References

American Association of State Highway and Transportation Officials (AASHTO). (2020). Interim LRFD Bridge Design Specifications. 9th ed., Washington, D.C., USA.

Bergado, D., Anderson, L., Miura, N., & Balasubramaniam, A. (1996). Soft ground improvement in lowland and other environments, ASCE Press, New York.

Circulado, U., & Lorenzo, G. (2020). Large-scale prototype testing of a composite geosynthetics reinforced earth structure for riverbank slope protection using fine grained sandy soil. *Mindanao Journal of Science and Technology*, *18*(1), 67-92.

Climaco, B. (2019). Infra damage due to ompong soars to P49.9M. Retrieved from https://m.facebook.com/story/graphql_permalink/?graphql_id=UzpfSTk2NjY2MzAzMDEzOjEwMTU1OTI3MTI4ODI4MDE0

Elias, V., Christopher, B., & Berg, R. (2001). Mechanically stabilized earth walls and reinforced soil slopes: design & construction guidelines. FHWA-NHI-00-043, Federal Highway Administration, Washington, DC.USA.

GMA News. (2016). QRT: Riprap sa boundary ng Marikina at San Mateo, Rizal, gumuho. [Video File]. Retrieved from https://www.youtube.com/watch?v=VsT7jB2Y8TY.

GMA News. (2015). UB: Pundasyon ng 5 bahay na nakatayo malapit sa creek sa Caloocan, gumuho. Retrieved from https://www.youtube.com/watch?v=dGEkzLr6ypw.

Guler, E., & Ocbe, C. (2003). Centrifuge and full-scale models of geotextile reinforced walls and several case studies of segmental retaining walls in Turkey. *Emirates Journal for Engineering Research*, *8*(1), 15-23.

Hejazi, M., Sheikhzadeh, M., Abtahi, S., & Zadhoush, A. (2012). A simple review of soil reinforcement by using natural and synthetic fibers. *Journal of Construction and Building Materials*, *30*, 100-116.

Holtz, R., Christopher, B., & Berg, R. (1997). Geosynthetic Engineering. BiTech Publishers, Vancouver, British Columbia, Canada, 451.

Khan, I., & Saran, S. (2006). A model study in metallic strip-reinforced earth wall. *Malaysian Journal of Civil Engineering*, *18*(1), 38-45.

Khan, R., Ali, S., & Riaz, M. (2024). Evaluation of design parameters for geosynthetic reinforced soil integrated bridge systems. *Frontiers in Materials*, *11*, Article 1454201. Retrieved from https://www.frontiersin.org/articles/10.3389/fmats.2024.1454201/full

Koerner, R., & Koerner, G. (2011). The importance of drainage control for geosynthetic reinforced mechanically stabilized earth walls. *Journal of GeoEngineering*, *6*(1), 3-13.

Koerner, R. (1998). Designing with Geosynthetics (5th Ed.). Pearson Prentice Hall, Upper Saddle River, NJ 07458: Person Education, Inc.

Morsy, A., Zornberg, J., Christopher, B., & Leshchinsky, D. (2020). Empirical model for predicting lateral displacements in geosynthetic-reinforced soil walls with segmental block facings. Geo-Institute of ASCE. Retrieved from https://sites.utexas.edu/zornberg/files/2022/03/Morsy_Zornberg_Christopher_Leshchinsky_2020.pdf

Pokharel, S., Han, J., Parsons, R., & Qian, Y. (2009). Experimental study on bearing capacity of geocell-reinforced bases. Bearing Capacity of Roads, Railways and Airfields – Tutumluer & Al-Qadi (eds), 1159-1166.

Rawi, O., & Abade M. (2017). Design of geo-synthetic retaining walls as an alternative to the reinforced concrete walls in Jordan. *American Journal of Engineering Research, 6*(12), 301-312.

Reddy, M., Reddy, K., & Asadi, S. (2018). An experimental study on combination of geosynthetic material with sand for evaluation of shear strength parameters. *International Journal of Pure and Applied Mathematics, 119(*4), 1779-1786. https://doi.org/10.13140/RG.2.2.28463.18086

Sharma, A., Yadav, R., & Singh, B. (2024). Use of geosynthetic materials as soil reinforcement: A review of engineering applications and future prospects. *Innovative Infrastructure Solutions, 9*, 50. Retrieved from https://link.springer.com/article/10.1007/s44290-024-00050-6

Sharma, M., & Goliya, H. (2014). Design and economic analysis of reinforced earth wall. *International Journal of Emerging Trends in Engineering and Development, 4*(6), 172-188.

Shirsath, M., & Choudhari, K. (2018). Role of Geosynthetics in sustainable development. *International Journal of Academic Research and Development, 3*(2), 89-93.

Soleimanbeigi, A., Likos, W., Tanyu, B., & Aydilek, A. (2016). Recycled materials as backfill for mechanically stabilized earth walls (Thesis), University of Wisconsin-Madison, USA.

Szymanski, A., Mazurek, A., & Sadowski, Ł. (2021). Performance comparison of geodrain and gravel drainage layers embedded in a horizontal plane. *Archives of Civil Engineering, 67*(4), 119–135. Retrieved from https://www.researchgate.net/publication/355479303